

Coherent bremsstrahlung by electrons and positrons in silicon and niobium crystals

G. L. Bochek, I. A. Grishaev, N. P. Kalashnikov, G. D. Kovalenko,
V. L. Morokhovskii, and A. N. Fisun

Physico-technical Institute, Ukrainian Academy of Sciences

(Submitted March 21, 1974)

Zh. Eksp. Teor. Fiz. 67, 808–815 (August 1974)

The experimental dependences of the intensities of secondary electrons and positrons of energy E on the orientation angle θ are compared with Born-approximation calculations for silicon and niobium crystals ($E = E_0 - \omega$, E_0 is the initial beam energy, ω is the emitted-photon energy, and $\hbar = c = 1$). Satisfactory agreement between the experimental data for electrons and positrons in the silicon crystal is obtained in the first Born approximation at orientation angles $\theta \geq 10^{-3}$ rad. The effect of electron and positron channeling is observed at angles $\theta < 10^{-3}$ rad. There is a discrepancy between the experiments and the first-Born-approximation calculations for the niobium crystal. The discrepancy can be resolved by taking the bremsstrahlung into account in the eikonal approximation. A description of the coherent bremsstrahlung in the first Born approximation may be insufficient for crystals with $Z \sim 40$ in the energy range under consideration. Allowance for the dynamics of the process leads to a decrease of the bremsstrahlung interference peaks and to a shift of the principal peaks towards larger angles.

1. INTRODUCTION

Interference phenomena^[1–3] connected with the periodic structure of the crystal appear in the bremsstrahlung spectrum of relativistic charged particles in single crystals. Experimental results on coherent bremsstrahlung of electrons were obtained with cyclic^[4, 5] and linear^[6, 7] accelerators for diamond and silicon crystals. The large divergence of the primary-particle beam (10^{-3} rad) and the background radiation greatly influence the coherent effects at small crystal disorientation angles, and make the comparison of the theoretical and experimental results in this angle region difficult. In addition, the Born approximation can no longer be used to describe coherent bremsstrahlung when the initial particle energy is increased, since the intensity at the maximum of the interference radiation, obtained with the aid of perturbation theory^[1–3], increases without limit with increasing energy, and this leads to violation of unitarity^[8, 9]. In this connection it is necessary to consider coherent bremsstrahlung in a crystal without the use of the Born approximation, and with greater accuracy than in the wide Weizsäcker-Williams method. Allowance for the second Born approximation^[10] in the theory of coherent bremsstrahlung leads to a dependence of the emission cross section on the sign of the charge. At the same time, the fact that perturbation theory is no longer valid for the description of elastic scattering of fast charged particles in a crystal^[11], and the effect of channeling of relativistic electrons^[12] and positrons^[13, 14], call for a new formulation of the question of bremsstrahlung of electrons and positrons at small crystal-orientation angles. In light of these factors, interest attaches to a more correct comparison of the experimental results for coherent bremsstrahlung of electrons and positrons with the theory.

2. EXPERIMENTAL PROCEDURE AND RESULTS

The energy dependence of the bremsstrahlung cross section at a fixed angle of rotation of the crystal, and the measurement of the angular dependence of the bremsstrahlung cross section for a fixed energy, can be effected by two methods:

- 1) Determine the intensity and energy of the photons by measuring the production of electron-positron pairs with a converter, followed by a subsequent analysis.

2) Measure the intensity and energy of the secondary electrons after the emission of the photons.

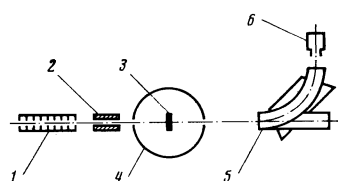
Each of these methods has advantages and shortcomings. Among the advantages of the second method is the rapid accumulation of the information, among the shortcomings is the decrease of the coherent effects as a result of scattering of the secondary electrons in the crystal target.

A comparison of the cross sections of the coherent bremsstrahlung of electrons and positrons becomes possible if one excludes effects connected with the characteristics of the beams, or if the contribution of these effects is the same for the electrons and positrons. In the present experiment we obtained beams of positrons and electrons with nearly equal characteristics.

The experimental setup is shown in Fig. 1. A positron beam^[15] obtained by converting the main electron beam was accelerated to an energy $E_0 = 1$ GeV and was directed to a crystal target secured in a goniometer. After emission of photons of energy ω , the secondary positrons of energy $E_0 - \omega$ were separated with a spectrometer and registered by an ionization chamber. To obtain an electron beam from the crystal, it is necessary to change the phase of the accelerating field and the polarities of the solenoid, of the lenses, and of the corrections. The measurements of the characteristics of the beams of the electrons and positrons have shown that this sequence of operations makes it possible to obtain beams whose parameters do not differ within the limits of the measurement errors.

From the point of view of obtaining minimum beam divergences, it is preferable to perform the experiment with a straight beam, but an adverse phenomenon appears, namely the presence of background particles in the working energy range. An appreciable decrease in the intensity of the background particles could be ob-

FIG. 1. Experimental setup:
1—accelerator, 2—collimator, 3—
crystal, 4—goniometer, 5—spec-
trometer, 6—ionization chamber.



tained by careful phasing of the sections of the accelerator and of the beam path, and subsequently by shortening the duration of the current pulse.

The goniometric system used in the experiment makes it possible to rotate the crystal about 2 mutually perpendicular axes and about the beam axis. The vertical rotation axis of the goniometer always remains normal to the beam. The accuracy of rotation about the goniometer axis is 5×10^{-5} rad, and around the beam axis it is 3.5×10^{-4} rad. The alignment of the crystallographic axes of the sample with the goniometer rotation axes was not worse than 10^{-3} rad. The goniometer was calibrated with an LG-55 laser and a long-focus optical system. The distance between the goniometer and the screen was 75 m. The calibration accuracy was $\sim 10^{-5}$ rad.

The single-crystal targets were secured in a clip. Three single crystals could be secured simultaneously in the clip. Preliminary orientation of the crystals was carried out by an x-ray procedure. The orientation of the targets relative to the clip was carried out also with the aid of a laser. The accuracy of the preliminary setting was 10^{-3} rad. The clip with the crystals was placed in the goniometer. Rotation around the beam axis was used to set the crystal in the beam and to align its crystallographic axes with the goniometer rotation axis.

The use of a multicrystal goniometer makes it possible to investigate coherent bremsstrahlung from several crystals at fixed beam parameters.

Silicon and niobium crystals were used in the experiment. Their principal characteristics are listed in the table.

Important factors in the experiment are the energy resolution and the vertical and horizontal angular acceptances of the spectrometer. The angular acceptances of the spectrometer were 6×10^{-3} rad in the horizontal plane and 10^{-3} rad in the vertical plane. The energy resolution was 0.5%.

The secondary electrons (positrons) were registered with an ionization chamber. The chamber signal was amplified and fed to the (y) input of an automatic recording potentiometer PDS-21. The other (x) input received a signal proportional to the crystal rotation angle. This yielded the orientation dependences of the secondary-electron (positron) yields. These dependences were subsequently reduced with a computer in accordance with the "Speedball" program. With this program, the graphic material was converted into numerical printouts which were compared with the theoretical calculations.

Figures 2 and 3 show the orientation dependences of the intensities of the secondary electrons and positrons for silicon and niobium crystals. The initial particle energy here and in the subsequent figures is $E_0 = 1$ GeV. The abscissas are the angles between the beam direction and the crystallographic axis (for silicon [110] in the (001) plane, for niobium [111] in the (112) plane), and the ordinates represent the ratio I/I_0 , where I is the intensity of the secondary electrons (positrons) as a function of the crystal rotation angle, while I_0 is the intensity of the secondary electrons and positrons from the disoriented crystal. The disorientation angle was 2.8×10^{-2} rad for silicon and 8×10^{-2} rad for niobium.

The errors connected with the uncertainty (on the order of 10^{-3} rad) of the direction of the rotation axis relative to the direction of the crystallographic axis, and

Crystal	Atomic number	Plane normal to the beam	Rotation axis	Thickness, μ	Thickness, rad. un. of length
Silicon	14	(110)	[001]	{ 640 190 150	{ 6.7 · 10 ⁻³ 1.99 · 10 ⁻³ 1.3 · 10 ⁻²
Niobium	41	(111)	[112]		

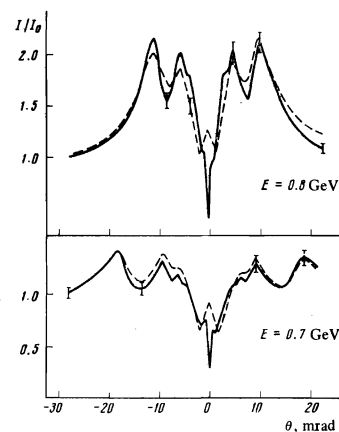


FIG. 2. Dependence of the yield of the secondary electrons and positrons on the angle between the beam direction and the crystallographic axis [110] in the (001) plane for the silicon crystal: dashed—electrons, solid—positrons.

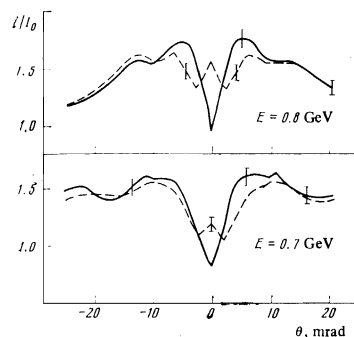


FIG. 3. Dependence of the yield of the secondary electrons and positrons on the angle between the beam direction and the crystallographic axis [111] in the (112) plane for niobium crystal: dashed—electrons, solid—positrons.

with the errors in the determination of the principal characteristics of the beam, were determined by averaging the series of diagrams obtained in different measurement runs, corresponding to definite values of the initial and secondary energy and also to the sign of the particle. The maximum deviations of the curves from the averaged curve did not exceed 5%.

3. ANALYSIS OF EXPERIMENTAL RESULTS

For our experimental conditions it is necessary to take into account the influence of the scattering of the primary and secondary particles on the coherent effect. The small angular acceptance of the spectrometer in the vertical plane makes it possible to take into account the influence of the particle scattering on the coherent bremsstrahlung only in the horizontal plane.

Figures 4 and 5 show the orientation dependences of the yield of the secondary electrons and positrons with energies 700 and 800 MeV for the silicon crystal. The initial electron energy is 1 GeV. The same figures show the orientation dependences with allowance for the scattering of the primary and secondary particles in the target. The rms multiple-scattering angle is given by

$$(\theta^2)^{1/2} = 2t^{1/2}E_0^{-1}, \quad (1)$$

where t is the thickness in radiation units of length, E_0 is the energy of the particle in GeV, and θ is the angle in mrad. Allowance for the multiple scattering leads to a decrease of the coherent effects and to a shift in the position of the coherent maxima towards larger angles.

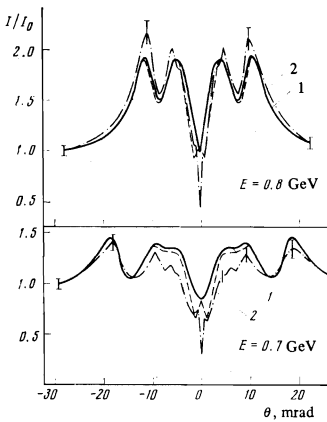


FIG. 4. Dependence of the yield of secondary positrons on the angle of orientation of the silicon crystal: 1—theory with allowance for multiple scattering of primary and secondary positrons, 2—experiment; dashed—fluence of the dependence of the multiple-scattering angle on the crystal orientation.

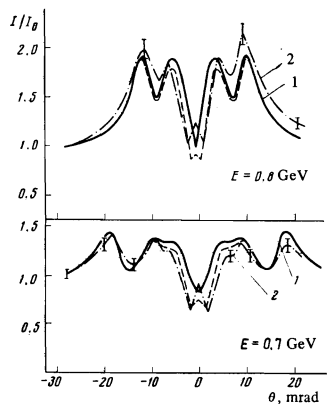


FIG. 5. Dependence of the yield of secondary electrons on the silicon crystal orientation angle: 1—theory with allowance for multiple scattering of primary and secondary particles, 2—experiment; dashed—fluence of the dependence of the multiple-scattering angle of the electrons on the crystal orientation.

For secondary electrons with energy $E = 700$ MeV, allowance for multiple scattering shifts the first coherent maximum by 10^{-3} rad.

Calculations for the niobium crystal differ only in allowance for the actual crystal structure. The crystal lattice is body-centered. Each cell contains 2 atoms. The structure factor of this lattice is

$$|S|^2 = 2(1 + \cos \pi(h+k+l)), \quad (2)$$

where h , k , and l are the Miller indices.

Ter-Mikaelyan^[16] has investigated the dependence of the scattering angle on the orientation of the beam of charged particles relative to the crystallographic axes. In later studies by others^[4-6], however, the rms multiple-scattering angle was assumed to be independent of the crystal orientation angle. When account is taken of the spectrometer characteristics (large angular acceptance in the horizontal plane and small acceptance in the vertical plane), even a slight dependence of the scattering angle on the crystal orientation leads to significant changes in the measured orientational dependences of the yielded secondary particles and positrons of fixed energy. The dashed lines in Figs. 4 and 5 show the influence of the dependence of the multiple-scattering angle on the orientation effects. The dependence of the multiple-scattering angle on the orientation for the electrons and positrons was determined experimentally. Allowance for the dependence of the multiple-scattering angle on the orientation angle for the electrons and positrons leads to a much better agreement between theory and experiment in the angle region $\theta > 10^{-3}$ rad^[16, 17].

The theoretical expressions for the cross section for the coherent bremsstrahlung in the Born approximation do not depend on the sign of the charge of the initial par-

ticle^[1-3]. A comparison of the experimental results of the coherent bremsstrahlung of the electrons and positrons yields information on processes that depend on the sign of the charge. It follows from the obtained experimental data that the orientation dependences for the electrons and positrons differ most strongly in the region $\theta \leq 10^{-3}$ rad. In the region $\theta > 10^{-2}$ rad, the orientation dependences for the electrons and positrons practically coincide. In the angle region $\theta < 10^{-3}$ rad one observes for the electrons an increase in the intensity of the secondary electrons, and for the positrons a decrease in the number of positrons. Figure 6 shows the orientational dependences of the yield of the secondary electrons and positrons for different silicon-crystal thicknesses. The range of angles where a difference is observed between the electrons and positrons coincides with the region of angles in which the effect of channeling of electrons and positrons is observed^[14]. Therefore, when coherent emission of fast charged particles is investigated in relatively thick single crystals ($L > L_0$), it is necessary to take into account the effects of the channeling on the process of bremsstrahlung. The length L_0 characterizes the minimum thickness of the single crystal over which the channeling regime is established:

$$L_0 \sim 2E_0(\kappa^2 + E_0^2\theta^2)^{-1}, \quad (3)$$

where $\kappa = me^2Z^{1/3}$ is the reciprocal screening radius.

If the angle at which the particle is emitted into the single crystal is less than the limiting channeling angle

$$\theta_{cr} < \theta_{cr} = (2\pi Ze^2/\kappa a^2 E_0)^{1/4}, \quad (4)$$

where Z is the atomic number of the single crystal and a is the lattice constant, then the overwhelming number of beam particles is captured in the channeling regime. The wave function of the channelled particle in the single crystal differs greatly from the incident plane wave, and near the lattice sites the wave function of the positron attenuates exponentially^[18]. In this case the bremsstrahlung probability decreases strongly, since the channeling leads to a suppression of processes with small impact parameters. Therefore a narrow minimum appears in the distribution of the intensity of the interference bremsstrahlung. The angle width of this minimum is determined by the limiting channeling angle (4). The main contribution to the bremsstrahlung in the forward direction is made by positrons that are not captured into the channeling regime; the fraction of these positrons is

$$\frac{N_0 - N_{chan}}{N_0} \sim \left(\frac{\kappa}{E_0} \frac{\pi}{4Ze^2} \right)^{1/2} \ll 1. \quad (5)$$

The contribution made to the coherent bremsstrahlung by the channelled particles is small.

For electrons it is also possible to realize a channeling regime in the angle range $\sim \theta_{cr}$. However, the electrons move in the channeling regime predominantly near the lattice sites. Therefore a peak is produced in the spectrum of the coherent bremsstrahlung of the electrons in the forward direction at zero entrance angle (the peak width is $\lesssim \theta_{cr}$). The height of this peak is smaller than the depth of the minimum for positrons of the same energy. With increasing particle entrance angle relative to the crystallographic plane, the bremsstrahlung spectrum goes over into the usual spectrum of the interference bremsstrahlung^[9].

Figure 7 shows the orientational dependences of the yield of the secondary electrons and positrons, as well as the theoretical values in the Born approximation,

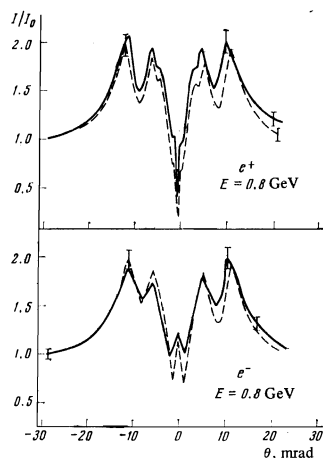


FIG. 6. Influence of the crystal thickness on the orientational dependence of the yield of secondary electrons and positrons: solid curve—thickness of silicon crystal $t = 6.7 \times 10^{-3}$ rad. un., dashed— $t = 1.99 \times 10^{-3}$ rad. un.

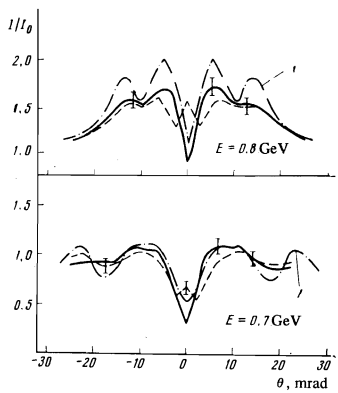


FIG. 7. Orientational dependences of the yield of secondary electrons and positrons for niobium crystal: 1—theory, solid curve—positrons, dashed—electrons.

with allowance for the particle scattering, for niobium single crystals. For secondary particles with energy $E = 800$ MeV, a discrepancy is observed between theory and experiment. With increasing secondary-particle energy ($E = 700$ MeV), the theory describes well the experimental results. This discrepancy may be due to the dynamic shortening of the coherence length of the bremsstrahlung when fast charged particles interact with single crystals, which leads to the suppression of the maxima of the interference bremsstrahlung by a factor

$$\left\{ 1 + \frac{Ze^2}{a} \frac{E_0(E_0 - \omega)}{m^2 \omega} \right\}^{-1}$$

and also to a shift of the principal maxima towards larger angles by an amount [8] $\Delta\theta \sim Ze^2/a\kappa$.

¹B. Ferretti, Nuovo Cimento **7**, 118, 1950.

²M. L. Ter-Mikaelyan, Zh. Eksp. Teor. Fiz. **25**, 296 (1953).

- ³H. Uberall, Phys. Rev. **103**, 1055, 1956.
- ⁴G. Barbiellini, G. Bologna, G. Diambrini, G. P. Murtas, Nuovo Cim. **28**, 435, 1963. G. Bologna, G. Lutz, H. D. Schulz, U. Timm, and W. Zimmermann, Nuovo Cim. **42**, 844, 1966.
- ⁵R. O. Avakyan, A. A. Aramganyan, L. G. Arutyunyan, G. A. Vartapetyan, L. Ya. Kolesnikov, and R. M. Mirzoyan, Tr. Mezhdunarodnoi konferentsii po apparatu v fizike vysokikh energii (Proc. Internat. Conf. on Apparatus in High-Energy Physics), Dubna (1971), p. 746.
- ⁶V. G. Gorbenko, Yu. V. Zhebrovskii, L. Ya. Kolesnikov, I. I. Miroshnichenko, A. L. Rubashkin, P. B. Sorokin, and V. F. Chechetenko, ibid., p. 738.
- ⁷I. A. Grishaev, V. I. Kasilov, G. D. Kovalenko, V. L. Morokhovskii, and A. N. Fisun, in: Voprosy atomnoi nauki i tekhniki, seriya Fizika vysokikh energii (Problems of Atomic Science and Engineering, Series on High-Energy Physics), KhFTI 72-45, Khar'kov (1972), p. 22.
- ⁸B. Ferretti, Nuovo Cim., **7B**, 225, 1972.
- ⁹N. P. Kalashnikov, Zh. Eksp. Teor. Fiz. **64**, 1425 (1973) [Sov. Phys.-JETP **37**, 723 (1973)].
- ¹⁰A. I. Akhiezer, P. I. Fomin, and N. F. Shul'ga, ZhETF Pis. Red. **13**, 713 (1971) [JETP Lett. **13**, 506 (1971)].
- ¹¹N. P. Kalashnikov, É. A. Koptelov, and M. I. Ryazanov, Zh. Eksp. Teor. Fiz. **63**, 1107 (1972) [Sov. Phys.-JETP **36**, 583 (1973)].
- ¹²H. Kumm, E. Bell, R. Sizmann, and H. J. Kreiner, Radiation effect, **12**, 53, 1972.
- ¹³R. L. Walker, B. L. Borman, R. C. Der, T. M. Kavanagh, and J. U. Khan, Phys. Rev. Lett. **25**, 5, 1970.
- ¹⁴V. L. Morokhovskii, G. D. Kovalenko, I. A. Grishaev, A. N. Fisun, V. I. Kasilov, B. I. Shramenko, and A. N. Krinitsyn, ZhETF Pis. Red. **16**, 162 (1972) [JETP Lett. **16**, 112 (1972)].
- ¹⁵V. I. Artemov, I. A. Grishaev, A. N. Dovbnya, L. Ya. Kolesnikov, N. I. Mocheshnikov, V. V. Petrenko, P. V. Sorokin, S. G. Tonapetyan, A. N. Fisun, and B. I. Shramenko, Mezhdunarodnaya konferentsiya po uskoritelyam chastits vysokikh energii (Internat. Conf. on High Energy Particle Accelerators), Erevan, No. 1 (1970), p. 493.
- ¹⁶M. L. Ter-Mikaelyan, Zh. Eksp. Teor. Fiz. **25**, 289 (1953).
- ¹⁷N. P. Kalashnikov and E. A. Koptelov, Fiz. Tverd. Tela **15**, 1668 (1973) [Sov. Phys.-Solid State **15**, 1121 (1973)].
- ¹⁸N. P. Kalashnikov, Tr. 5th Vsesoyuznogo soveshchaniya po fizike vazimodeistviya zaryazhennykh chastits s monokristallami (Proc. 5th All-Union Conf. on Physics of Charged-Particle Interaction with Single Crystals, Moscow, 1973).

Translated by J. G. Adashko
93